HHS Public Access

Author manuscript

Nanoscale. Author manuscript; available in PMC 2018 June 29.

Published in final edited form as:

Nanoscale. 2017 June 29; 9(25): 8684–8694. doi:10.1039/c7nr03096g.

Site-Specific Conjugation of Antibody on Gold Nanoparticle Surface for One-Step Diagnosis of Prostate Specific Antigen with Dynamic Light Scattering

Nur Mustafaoglu[a], **Tanyel Kiziltepe**[a,c], and **Basar Bilgicer**[*,a,b,c,d,e,f]

[a]Department of Chemical and Biomolecular Engineering

[b]Department of Chemistry and Biochemistry

[c]Advanced Diagnostics and Therapeutics

[d]Mike and Josie Harper Cancer Research Institute

[e]Center for Rare & Neglected Diseases

[f]ND Nano Center for Nano Science and Technology, University of Notre Dame, University of Notre Dame, Notre Dame, IN 46556, USA

Abstract

Small dimensions of gold nanoparticles (AuNPs) necessitate antibodies to be immobilized in an oriented fashion in order to conserve their antigen binding activity for proper function. In this study, we used the previously described UV-NBS method to site-specifically incorporate thioctic acid (TA) functionality into antibodies at the conserved nucleotide-binding site (NBS). Modified antibodies were immobilized on AuNP surface in an oriented manner utilizing the newly incorporated TA functionality while maintaining antibody structure and activity. The resulting antibody functionalized AuNPs via the UV-NBS method demonstrated significantly enhanced antigen detection capabilities and improved antigen detection sensitivity with high level of selectivity when compared to other commonly used AuNP functionalization methods. Our results demonstrate that the limit of detection (LOD) for AuNPs functionalized via the UV-NBS method was 55 pM PSA, which is 40, 851, and 5873-fold improved over the other immobilization methods: EDC-NHS, thiol reduction, and ionic interaction, respectively. Consequently, the UV-NBS method provides a universal, site-specific functionalization method that generates highly sensitive and more stable antibody functionalized AuNPs that is amenable to any available detection and treatment assay with potential significant implications.

INTRODUCTION

Implementation of gold nanoparticle (AuNP)/antibody conjugates in biomedical applications including diagnostics[1–3], therapeutics[4–7], and theranostics[8,9] as biochemical sensors,

[*]**Corresponding Author:** Basar Bilgicer, Associate Professor, Department of Chemical and Biomolecular Engineering, Department of Chemistry and Biochemistry, Advanced Diagnostics & Therapeutics Initiative, Mike and Josie Harper Cancer Research Institute, Center for Rare & Neglected Diseases, Center for Nano Science and Technology, University of Notre Dame, 205 McCourtney Hall, Notre Dame, IN 46556-5637, Voice: 574-631-1429, Fax: 574-631-8366, bbilgicer@nd.edu.

enzyme enhancers, nanoscale building blocks and immunohistochemical probes, is becoming more common practice.[10,11] Various shapes (nanospheres, nanorods, and nanocubes) and sizes (2 to 150 nm) of AuNPs give them unique electrical, physical, mechanical and optical properties.[12–15] AuNP's strong light absorption and scattering abilities in both visible and infrared region adjustable via size, shape and dielectric constant make them relevant to be used in imaging and sensing.[16–19] Antibody provides the necessary specificity and sensitivity in such applications, therefore methods for functionalization of the AuNP surfaces with antibodies is required for implementation of AuNPs in selective and sensitive diagnostic applications.[20–22] The limited number of antibodies (~10 nm) that can be immobilized on such small surface area of AuNP (78.5 nm^2 for 5 nm AuNPs), necessitate oriented immobilization of antibodies on AuNP surface. Otherwise, most of the randomly oriented antibodies lose their function resulting in many of the AuNPs without any functional antibody on their surfaces to recognize antigens; thus, those AuNPs without any functional antibody drastically reduce the sensitivity of biosensing application. Therefore, functionalization of antibodies without inhibiting antigen binding activity requires the conjugation to be site specific in order to obtain stable and active antibody immobilization on AuNP surface ensuring enhanced detection of target analytes.

The nature of AuNP surface chemistry promotes easy and controlled attachment of molecules especially those with thiol functionalities.[23–25] The most common strategies for labeling AuNPs with proteins are ionic (electrostatic) interactions, EDC/NHS method, and antibody thiol (disulfide bond) reduction.[26,27] The ionic interaction strategy is based on the attraction between the charged surfaces of two reacting partners. Due to positively charged residues, such as lysine and arginine available in their sequences, antibodies can readily interact with the negatively charged citrate stabilized AuNPs.[26,28] Although ionic interaction strategy is simple and time saving, this method can be easily influenced by factors like pH, ionic strength, and nature of solvent. Furthermore, predictably, the stability of the antibody functionalized AuNPs produced via ionic interactions is very poor.[29] More importantly, the electrostatic coupling generates AuNPs with randomly oriented antibodies on their surfaces, which causes hindrance of antigen binding site (ABS) and consequently result in loss of antigen-binding activity. The other methods also have similar drawbacks. EDC/NHS method uses the ε-amine groups of lysine residues for attachment to carboxyl group of reaction partner, are located at varying positions on the surface of the antibody. This method can reduce the antibody activity due to potential hindrance of the ABS as a result of conjugation at an ABS residue or random orientation of antibody on the AuNP surface.[30,31] Thiol reduction method requires harsh chemical conditions, which impacts the antibody tertiary structure and reduce its activity.[20,23,32] Furthermore, low sensitivity levels, short storage time, and poor stability are the other consequences that originate from these commonly used methods for generating antibody functionalized AuNPs. In this paper, we describe how we overcome these limitations by using site-specific covalent functionalization of antibody with thiol moieties prior to immobilization on AuNPs.

We have previously reported the UV-NBS, UV-NBS^{Biotin} and UV-NBS^{Thiol} methods that have been developed in our laboratory as universal methods for site-specific functionalization of antibody and Fab fragments, as well as oriented immobilization.[33–38] These methods utilize the nucleotide-binding site (NBS) of antibody as a binding pocket for

conjugation of small indole molecules such as indole 3-butyric acid (IBA) and tryptamine. Although the NBS has no known function, it is a highly conserved region located in the variable domain of the Fab fragment.[34,36] We characterized and reported this site in our previous publications using *in silico* methods to identify the four critical residues that make up the site; two tyrosine residues (Tyr42 and Tyr103) on the light chain (V_L) and one tyrosine (Tyr103) and one tryptophan (Trp118) residue on the heavy chain (V_H).[34,39] Our group has identified that small indole structured molecules typically have a moderate binding affinity to the NBS with a K_d = 1–8 μM.[34,39] The UV-NBS method utilizes UV energy to initiate a reactive radical driven reaction between the indole molecule and the NBS,[34] which provides an opportunity to produce functionalized antibodies and fab fragments with various functional groups such as affinity tags, imaging molecules, chemotherapeutics and peptides.[33–38] In multiple publications, we established that the UV-NBS method can be used to functionalize antibodies without unfavorably impacting their antigen binding activity. Furthermore, we also demonstrated many utilities that the NBS can provide in a variety of applications beyond covalent linking such as oriented immobilization,[35,36] enhanced antigen detection,[35,37,38] as well as inhibition of allergic reactions[39–41].

In the present study, we demonstrate an application for oriented immobilization of UV-NBS functionalized antibodies onto AuNP surfaces for enhanced antigen detection. We used the affinity of tryptamine molecule to the NBS for site-specific functionalization of antibodies with thiol moieties (Fig. 1). To demonstrate the utility of the UV-NBS method for antibody immobilization on AuNPs, we used a prostate specific antigen (PSA) detection system to evaluate the antigen detection sensitivity, antigen recognition selectivity and limit of detection (LOD).[42,43] We synthesized tryptamine-EG_8-TA molecule in order to conjugate with two different anti-PSA antibodies; B731M and B728M via the NBS. TA functionalized antibodies were immobilized on AuNPs in an oriented manner via thiol-gold bond. To demonstrate the advantages of the UV-NBS method, we compared the antigen recognition sensitivity of the detection system with other AuNP functionalization methods; EDC-NHS method, thiol reduction, and ionic interactions.

MATERIALS AND METHODS

Materials

Tryptamine, hemoglobin, PBS and N,N-diisopropylethylamine (DIEA) were purchased from Sigma-Aldrich (St. Louis, MO). TCEP HCl and human serum was purchased from Thermo Scientific (Rockford, IL). Lipoamido-$dPEG_8$-acid and lipoamide-$dPEG_4$-acid were purchased from Quanta Biodesign (Powell, OH). HRP-conjugated IgG Fcγ specific goat anti-mouse antibody and HRP-conjugated mouse anti-human antibody were purchased from Jackson ImmunoResearch (West Grove, PA). Purified free prostate specific antigen (PSA), mouse anti-PSA (clone: B731M), and mouse anti-PSA (clone: B728M) were purchased from Meridian Life Science, Inc. (Memphis, TN). Sodium dodecyl sulfate (SDS) was purchased from Bio-Rad (Hercules, CA). Amplex Red Assay Kit was purchased from Invitrogen (Grand Island, NY). Human transferrin receptor protein fragment was purchased from Abcam (Cambridge, MA). Heat shock isolated bovine serum albumin (BSA), MES

Buffer, and Amicon ultra centrifugal filters (0.5 mL, 10K) were purchased from EMD Millipore (Billerica, MA). 15 nm Whatman Nuclepore Track-Etch Membrane was purchased from GE Healthcare Life Sciences (Pittsburgh, PA). 5 nm and 20 nm gold colloid nanoparticles were purchased from Cytodiagnostics (Ontario, Canada). Rituximab (chimeric human anti-CD20) was a gift from Dr. Alexander N. Starodub at the Indiana University Health Goshen Center for Cancer Care, IN.

Synthesis of tryptamine-EG_8-TA

To synthesize the tryptamine-EG_8-TA, tryptamine was conjugated to lipoamido-$dPEG_8$-acid in solution following HBTU activation in DMF with DIEA at room temperature (RT) for 4 h while stirring (Fig. S1). DMF was removed using rotate evaporation. The product was purified via RP-HPLC on a Zorbax C18 column, and characterized with MICRO-TOF MS. The calculated exact mass for tryptamine-EG_8-TA ($C_{37}H_{61}N_3O_{16}S_2$) was 771.38; found 772.42. The purity of the tryptamine-EG_8-TA was confirmed using RP-HPLC on an analytical Zorbax C18 column to be >95%.

Assessing antigen binding activity and Fc stability of the antibodies via ELISA

Antigen coated ELISA plate was generated incubating 10 nM PSA in high binding 96-well ELISA plate in PBS pH 7.4 for 2 h at RT. The antigen coated ELISA plates were washed to remove any unbound components using an automated plate washer (MDS Aquamax 2000, Sunnyvale, CA) for three times with 200 μL PBS including 0.05% Tween 20 at pH 7.4. The plate was then blocked with BSA blocking buffer including 5% BSA and 0.1% tween 20 in PBS pH 7.4 for 1 h. Various amount of UV energy (0 – 5 J/cm^2) was applied to antibodies in the presence of 300 μM tryptamine-EG_8-TA and was then incubated on the antigen-coated plate. After washing the plate for three times, the wells were incubated with 1:5000 dilution of HRP-conjugated anti-mouse secondary antibody (1 mg/mL stock concentration) in BSA blocking buffer 1 h. Amplex Red was used as the HRP substrate, then fluorescence intensity of the corresponding product was measured using a Molecular Devices SpectraMax M5 plate reader (ex. 570 nm, em. 592 nm). All experiments are performed in triplicate and the data represents means (± Standard Deviation) of triplicate experiments.

Photocrosslinking of tryptamine-EG_8-TA ligand to antibodies

We purchased all antibodies for photocrosslinking as purified antibodies with no protein stabilizer. Sodium azide, a very UV reactive preservative, was removed prior to UV exposure via spin concentrator with 10 kDa cut off. Antibodies were incubated with tryptamine-EG_8-TA (300 μM) for 1 h prior to UV exposure at RT. The amount of UV energy that is necessary to form a covalent bond between the ligand and the antibody was controlled using a Spectroline UV Select Series Crosslinker from Spectronics at the wavelength of 254 nm. Upon conjugation of antibodies with tryptamine ligand, excess ligand was removed via membrane filtration (0.5 mL, 10K).

Antibody immobilization on AuNPs

Stability of citrate stabilized AuNPs were tested in water, 1× PBS, 0.1× PBS and 0.01× PBS buffers by measuring their absorbance spectrum (Fig. S2). 0.01× PBS was found to be the

most appropriate buffer for AuNPs without causing any observed aggregation. We used 0.01× PBS as buffer for the rest of the experiments described in this article.

UV-NBS Method: TA functionalized antibodies incubated with gold nanoparticles (1:1 molar ratio) for 2 h while stirring at room temperature (RT).

EDC-NHS Method: Carboxylic acid modification of AuNPs was achieved by following the protocols described in a previous literature report.[44] Briefly, an aqueous solution of AuNP (90.8 nM) was mixed with SDS (0.0025%) and lipoamide-dPEG$_4$-acid (0.0024 mg/mL) under basic conditions for 16 h. Carboxylated AuNPs were purified by centrifugation (15000 rpm, 1 h). For antibody functionalization to AuNPs, we followed procedure from a literature report.[45] In brief, pellet of the carboxylated AuNPs were dissolved in MES buffer. EDC and NHS solutions were prepared freshly prior to incubation with AuNPs for 30 min. Final NHS and EDC to carboxylated AuNP molar ratios were 10 and 25, respectively. The resulting AuNP solution was incubated with antibodies for 2h.

Thiol reduction method: Antibody reduction reaction was performed by following the protocol from literature.[46] Briefly, 5 μL antibody (1 mg/mL), 5 μL TCEP solution (5 mM TCEP in solution) and 40 μL PBS pH 6.8 were mixed, and then incubated for 1 h at RT. Reduction of disulfide bonds of B731M and B728M were tested by running a 10% SDS-PAGE under non-reducing conditions (Fig. S3). Reduced half antibodies were observed around 75 kDa while intact antibodies observed around 150 kDa. To eliminate disulfide bond formation between half antibodies, reduction of the antibodies were performed at lower pH conditions, 6.8, in PBS. After determination of reduced antibody concentration by absorbance spectrum utilizing Beer-Lambert Law, reduced antibodies (60 nM) were immediately incubated with AuNPs (60 nM) for 2 h.

Ionic interaction method: 60 nM AuNPs were simply incubated with 60 nM antibody for 2 h at RT.

Purification of antibody functionalized AuNPs

Antibody functionalized AuNPs produced with four different methods were purified using liposome extruder purification (LEP) technique described in our previous report[47] utilizing 15 nm pore sized membrane, large enough to pass through non-functionalized antibodies and bare AuNPs and small enough to keep antibody functionalized AuNPs. During the purification process, buffer of the antibody functionalized AuNPs was changed with 1.5% BSA in 0.01× PBS. After purification step, concentrations of the antibody functionalized gold nanoparticles were determined using absorbance spectrum based on gold nanoparticle peak. The yield of the purified antibody functionalized AuNPs were found to be around 20–30%. The functionalized gold nanoparticles stored at 4°C until use.

Absorbance spectrum measurements of antibody functionalized AuNPs

Absorbance spectrum of both bare and the antibody functionalized gold nanoparticles were measured using a Molecular Devices SpectraMax M5 plate reader. All measurements were carried out in a quartz cuvette using a sample volume of 50 μL.

Dynamic light scattering (DLS) measurements

The hydrodynamic diameter of non-functionalized and antibody functionalized AuNPs were measured using DLS technique. Data was collected on a Brookhaven Instruments Corp. Zeta Plus instrument and was averaged from five 1 minute measurements. The lowest AuNP concentration that we can measure with the instrument was tested with varying AuNP concentrations in two different buffers: 0.01× PBS and 0.1% BSA in 0.01× PBS (Fig. S4). The rest of the DLS experiments were carried out using 50 μL of 5 pM antibody functionalized AuNPs in 0.1% BSA in 0.01× PBS. The refractive index (RI) value used for the AuNPs was 0.135.[26,48] Antigen samples both in buffer and spiked human serum samples were tested. Measurements were performed at 25°C in quartz fluorometer cell (3 mm, Z=15mm) using a sample volume of 50 μL.

RESULTS AND DISCUSSION

We used two different clones of anti-PSA monoclonal antibodies, B731M and B728M, which are specific to two different PSA epitopes, and functionalized them with tryptamine-EG_8-TA ligand via NBS photocrosslinking. UV-energy was utilized to initiate the site-specific photocrosslinking of the tryptamine-ligand at the NBS of both antibodies. The necessary UV energy, however, may potentially be destructive to the antigen-binding site as well as cause damage to the overall antibody structure. For this reason, we first assessed the effect of various levels of UV energy (0–5 J/cm^2) to both anti-PSA antibody clones in order to ensure that antigen binding activity and antibody structure stability were preserved at the UV energy that is used to form site-specific photocrosslinking of tryptamine-ligand to the antibody. A sandwich ELISA was performed to determine the impact of UV energy to the antigen binding activity and structure stability of antibody (Fig. S5). For this experiment, we first generated TA functionalized antibody samples utilizing a fixed amount of tryptamine-EG_8-TA (300 μM) and various levels of UV energy (0–5 J/cm^2). The functionalized antibodies were then incubated on PSA immobilized ELISA plates. We used an Fc specific HRP conjugated anti-mouse secondary antibody to determine Fc structure stability as well as antigen binding activity of antibodies post UV-exposure (Fig. S5B). According to the ELISA results, there is neither an observable reduction in antigen binding activity nor a detectable damage to antibody structure up to UV energies of 0.5 J/cm^2 for B728M and 2 J/cm^2 for B731M (Fig. S5A). We deduce a reduction in signal intensity at higher UV energies to be an indication of damage to antigen binding activity or to the antibody structure. These results indicate that B728M antibody clone is more sensitive to UV exposure than the B731M clone. This was expected since the UV wavelength chosen to perform the crosslinking reaction can have some impact on tryptophan, tyrosine, histidine, and cysteine residues at high energies. Thus, some antibodies including these residues closer to their surface where they are exposed to direct UV or in higher numbers, are more sensitive to UV-exposure.[49] Taken together, these results demonstrate that UV energies ≤0.5 J/cm^2 for B728M and ≤2 J/cm^2 for B731M can be utilized during photocrosslinking reactions with minimal impact on antigen binding activity and antibody structure stability. Furthermore, the results of ELISA experiments with B731M antibody are consistent with the results from our previous study for biotinylation of antibody utilizing the UV-NBS^{Biotin} method to oriented immobilization of antibodies for enhanced antigen detection.[35]

Therefore, based on the results of these experiments with the support of previous studies utilized the UV-NBS method[34–36], we selected to use 0.5 J/cm^2 and 1 J/cm^2 UV energies to form site-specific covalent photocrosslinking of tryptamine-EG$_8$-TA linker to B728M and B731M, respectively, without inversely affecting antigen binding or Fc activity.

Next, we synthesized antibody functionalized AuNPs utilizing TA modified antibodies. To achieve this, we mixed 1:1 molar ratio of each of the TA functionalized anti-PSA antibodies with 5 nm AuNPs (60 nM) in 0.01× PBS pH 6.8. Though the covalent gold-thiolate bond that form between double thiol groups of TA and AuNP surface, TA functionalized antibodies were conjugated to AuNPs in an oriented manner. We hypothesize that utilization of UV-NBS method will provide more controllability over both site-specific conjugation of antibodies via the NBS and oriented immobilization of them on AuNP surface; thus, will yield more stable and active antibodies immobilized on AuNPs compared to other commonly used methods. For comparison, we also prepared AuNPs that are functionalized with anti-PSA antibodies utilizing three other common methods: EDC-NHS, thiol reduction and ionic interaction, to compare with the UV-NBS method in terms of antibody immobilization on AuNPs and antigen recognition sensitivity.

For ionic interactions method, we simply mixed antibodies with gold nanoparticles and allowed them to non-covalently associate with each other. For thiol reduction method, we used *tris*(2-carboxyethyl)phosphine (TCEP) to reduce antibody's disulfide bond at the hinge region to reduce the antibodies into two halves. The half antibodies were then immobilized on AuNPs utilizing the thiol-gold covalent conjugation. We also used EDC-NHS, which is the most commonly used method for the antibody immobilization on various surfaces including gold, for generating antibody modified AuNPs utilizing ε-NH_3^+ groups of the lysine side-chains of antibodies. For this method, we first needed to modify AuNPs with carboxylic acid groups, and then carboxylated AuNPs were functionalized with anti-PSA antibodies utilizing EDC-NHS chemistry. AuNPs functionalized with anti-PSA antibodies with all four different methods were purified by using LEP technique[47], which was previously developed in our laboratories. Using the LEP technique, non-functionalized antibodies and bare AuNPs were separated from antibody modified AuNPs via a 15 nm membrane. Conjugation yield of antibodies on AuNPs surface was calculated by measuring concentrations of the pure antibody functionalized AuNPs samples and compared with the initial AuNPs concentration, and found ~22%, 30%, 25%, and 27% for the UV-NBS, EDC-NHS, ionic interaction, and thiol reduction methods, respectively. After the conjugation step using any of the methods, during the purification step, the reaction buffer, 0.01× PBS pH: 6.8, was changed with BSA blocking buffer to block non-functionalized surfaces on AuNPs with BSA for improved stability and resistance to aggregation.

To confirm the antibody functionalization of AuNPs, absorbance spectra of gold nanoparticles were measured before and after the antibody functionalization reaction. Fig. 2 demonstrates the changes in the absorbance spectra of AuNPs after functionalization with antibodies utilizing four different methods: UV-NBS, EDC-NHS, thiol reduction and ionic interaction. Prior to the antibody functionalization, the citrate-stabilized 5 nm AuNPs exhibit a plasmon resonance peak at 522 nm (black line). Replacing the citrate with antibodies and BSA as a block agent utilizing various methods causes a slight red-shift of the AuNP

plasmon resonance (1–3 nm) (Table S1). This slight peak shift is attributed to antibody immobilization on AuNPs surface since it is expected that antibody functionalized AuNPs would have a larger volume, which results in ~2 nm shift on its absorbance spectrum. Therefore, these absorbance spectra illustrate that two sets of AuNPs were successfully functionalized with two different antibodies, B731M (Fig. 2A) and B728M (Fig. 2B), utilizing all four immobilization methods without causing any aggregation. Furthermore, we measured the size of the AuNPs before and after antibody functionalization, and compare them with the size of antibodies (Fig. 2C). Due to the adhesion of BSA (~4 nm) around the surface of AuNPs (5 nm), the hydrodynamic diameter of BSA blocked AuNPs appears to be ~12 nm in BSA blocking buffer. Thus, it is predicted that the hydrodynamic diameter of antibody functionalized AuNPs becomes ~25 nm after functionalization of antibodies with the size of ~10 nm around the 5 nm AuNPs surface. We achieved the expected ~25 nm hydrodynamic radius for the antibody functionalized AuNPs with both the UV-NBS and EDC-NHS functionalization methods. A smaller hydrodynamic radius, ~20 nm, of antibody functionalized AuNPs was observed with the thiol reduction method, which was an expected result since only half of the antibodies were used to conjugate on AuNPs in this method. Ionic interaction method, however, also yield smaller conjugated AuNPs. This result may be observed due to the double population of samples: functionalized AuNPs (~25 nm) and non-functionalized AuNPs (~12 nm) or antibodies (~10 nm). Since ionic interaction method does not include any covalent conjugation of antibodies to AuNPs, providing unstable products with the possibility of antibody falling off from the AuNPs surface, it is likely to observe free AuNPs and antibodies over time. As an additional characterization of antibody functionalized AuNPs, number of antibody per AuNPs for each conjugation method was calculated by analyzing antibody functionalized AuNPs on size exclusion column (SEC), and identified to be 3.5±0.6, 7.8±0.3, 7.6±1.4, and 4.8±0.5 for the UV-NBS, EDC-NHS, thiol reduction, and ionic interactions, respectively (Fig S6).

To investigate the antigen binding sensitivity of the antibody functionalized AuNPs, varying concentrations of PSA (0–200 nM) were incubated with the mixture of two different clones of anti-PSA antibodies that are specific to two different PSA epitopes. Once the mixture of antibodies on gold nanoparticles associated with the antigen, they formed larger clusters depending on the antigen concentration (Fig. 3A). These clusters are easily detectable via DLS. As expected, utilization of only one kind of antibody on AuNPs, however, did not form clusters; thus, the size of the nanoparticles did not change upon incubation with increasing concentrations of PSA. We performed DLS experiments for determining the antigen recognition sensitivity of antibody functionalized AuNPs that were prepared using four different antibody immobilization methods (Fig. 3B,C,D,E). The antigen binding sensitivity of the antibody functionalized AuNP systems were determined with the coefficient of the natural logarithm from the linear part of the regression line (Fig. 3F and Fig. S7). The UV-NBS method demonstrated 5.1, 4.4, 3.2-fold higher antigen recognition sensitivity compared to ionic interaction, thiol reduction, and EDC-NHS, respectively. The size increment of the clusters with the UV-NBS method is higher than three other immobilization methods. Even though the UV-NBS provides lesser amount of surface immobilized antibody (~3.5) per AuNP compared to other methods (Fig. S6), antigen detection efficiency was significantly higher, demonstrating that the UV-NBS method yields

enhanced preservation of antigen binding activity per surface immobilized antibody. Thus, these results indicate that the UV-NBS method yields stable AuNPs functionalization with higher numbers of active antibodies on the AuNP's surface than other methods.

Furthermore, we determined the limit of detection (LOD) for PSA utilizing DLS measurements of cluster formations with all antibody-functionalized methods. To calculate the LOD values, we used the linear part of the logarithmic regression line from graph plotted using the DLS measurements vs analyte concentration (Fig. 3F and Fig. S7). The LOD was determined as the PSA concentration for each functionalization method at 3 standard deviations from the mean of the zero PSA standard.[50] The UV-NBS provided a significant improvement to the LOD for PSA compared to three other functionalization methods (Table 1). With 55 pM LOD for PSA detection, the UV-NBS method represents 40-, 851-, and 5873-fold lower value than the LOD of EDC-NHS, thiol reduction, and ionic interaction methods, respectively. This is a direct indication that UV-NBS method achieved significantly more active immobilized antibodies on AuNP surface than any other antibody functionalization technique tested.

We also tested the antigen binding sensitivity of the antibody functionalized AuNPs using PSA samples in human serum (Fig. 4). For this purpose, human plasma from healthy subjects were spiked with increasing concentrations of PSA, and then antibody functionalized AuNPs via the UV-NBS method was used to determine free PSA in human serum. Diameter of the cluster formation increased with increasing concentrations of PSA in the samples; which was indicative of highly sensitive detection of the antigen in biological samples. We calculated the detection limit for PSA in human serum to be ~4 pM using the linear part of the logarithmic regression line from graph ($y=12.8\ln(x)+80.15$) (Fig. S8). These results mirror those we obtained from the PSA samples that were in 0.1% BSA as obtained using AuNPs prepared using UV-NBS method. Therefore, combined these results established that antibody functionalized AuNPs provides a highly sensitive platform for rapid detection of antigens without any need of high-tech instrumentation or complex experimental methods.

Additionally, we assessed the antigen binding ability and the Fc stability of AuNP conjugated antibodies via a sandwich ELISA assay. The ELISA experiments were performed for two different antibodies, B731M and B728M, on AuNPs utilizing four different antibody immobilization methods (Fig. 5C). For this experiment, the antibody functionalized AuNPs were incubated on PSA (10 nM) immobilized ELISA plates for 1 h, and then an HRP conjugated Fc specific goat anti-mouse secondary antibody was used to detect the Fc region of the antibodies on AuNP's surface. Amplex Red was used as an HRP substrate to form fluorescent product for quantification purposes. The ELISA results validate that utilizing UV-NBS method for immobilization of antibodies on AuNPs provide better antigen binding activity and Fc region stability comparing to other commonly used functionalization methods (Fig. 5). The antigen binding activity and Fc structural stability of antibodies post immobilization on AuNPs were determined with the coefficient of the natural logarithm from the regression line. The UV-NBS method demonstrated 1.3-, 1.4-, and 4.2-fold for B731M (Fig. 5A) and 1.3-, 1.3-, 2.5-fold for B728M (Fig. 5B) higher antigen recognition and Fc fragment stabilization compared to ionic interaction, EDC-NHS

and thiol reduction methods, respectively. These quite similar results indicate the reproducibility of the UV-NBS method with higher quality. Predictably, thiol reduction method appeared to achieve the lowest antigen binding and Fc stability results due to secondary antibody's inability to recognize the disulfide reduced Fc fragments with only one heavy chain. It is also worth mentioning that, ionic interactions method appears to achieve higher activity than EDC-NHS method, which is inconsistent with the DLS experiments. We predict that the washing steps with washing buffer, 0.05% Tween 20 in PBS, in the ELISA experiment cause the separation of antibodies from AuNPs. Antibodies bound to the antigen that is immobilized on the ELISA surface, will remain attached during the washing step whereas AuNPs will be washed away, and that results with better antigen binding and Fc recognition of free soluble antibodies without steric hindrance of AuNPs. This outcome is also consistent with the result of previous DLS experiment (Fig. 2C) showing the smaller size of antibody functionalized AuNPs generated via ionic interactions, indicating two separate populations of AuNPs and antibodies in the sample. Results of both ELISA and DLS experiments performed in this study display the major drawback, instability, of the ionic interactions method, indicating that it is not a suitable method to functionalized antibodies on nanoparticles for diagnostic applications. Taken together, the results demonstrate that the UV-NBS method provides the highest retained activity of immobilized antibodies on AuNPs without causing any damage on their Fc fragments.

Next, we investigated the specificity of the antibody functionalized AuNPs generated via the UV-NBS method. For this experiment, we used various proteins such as bovine serum albumin (BSA) (Fig. 6A), transferrin (Fig. 6B) and hemoglobin (Fig. 6C), all of which may be found in high concentrations in body fluids; typical serum albumin concentration is 45 g/L[51], transferrin concentration is 3.07 g/L[52], and hemoglobin concentration is 123 – 157 g/L[53], instead of PSA. Predictably, utilization of those proteins instead of PSA as a target molecule did not form clusters with AuNPs that are functionalized with PSA specific antibodies (Fig. 6). These results indicate the high specificity of the UV-NBS detection method.

The specificity of the antigen detection with antibody functionalized gold nanoparticles utilizing the UV-NBS method was further evaluated. In this case, we used a non-PSA specific antibody, Rituximab, to immobilize on AuNPs surface utilizing UV-NBS method instead of an anti-PSA antibody (Fig. 7). Then, using DLS, we observed if any clusters would form with AuNPs of Rituximab, an anti-CD20 antibody, and one of the anti-PSA antibodies upon addition to PSA. Firstly, we confirmed the Fc stability of Rituximab antibody upon various amounts of UV energy prior to use of UV-NBS method for immobilization on AuNPs (Fig. S9). The results demonstrate that optimal UV energies for functionalization of tryptamine-EG_8-TA ligand without causing any damage on Fc fragment are 0–2 J/cm^2. By comparing those results with our previous studies[33,35], we decided to perform the photocrosslinking reaction of Rituximab antibody with tryptamine-EG_8-TA ligand at 1 J/cm^2. TA functionalized Rituximab antibody was then used to immobilize on AuNPs. Rituximab functionalized AuNPs were mixed with either B731M (Fig. 7A) or B728M (Fig. 7B) antibodies, which are immobilized on AuNPs surface, to test their cluster forming abilities in presence of PSA in the sample by measuring their size by DLS. The

results confirmed that one of the anti-PSA antibodies targeting the PSA accompanied with a non-specific antibody, Rituximab, on AuNP was not sufficient to form clusters.

Next, we further demonstrate the antibody functionalization of AuNPs for PSA detection via the UV-NBS method utilizing using 20 nm AuNPs instead of 5 nm AuNPs. Absorbance spectra confirm the successful modification of 20 nm AuNPs with B731M and B728M antibodies utilizing all four immobilization methods without causing any aggregation (Fig. S10). In the absorbance spectra of the functionalized AuNPs, there are only 2 nm, a slight red-shift, of the AuNP plasmon resonance for all methods indicating the larger volume of AuNPs post antibody functionalization (Table S2). The antigen binding sensitivity of antibody functionalized 20 nm AuNPs show similar trends compared to antibody functionalized 5 nm AuNPs (Fig. S11). The UV-NBS method is the leading method for antibody functionalization of both 5 nm and 20 nm AuNPs yielding the highest sensitivity for PSA detection with the lowest LOD, followed by EDC-NHS, thiol reduction and ionic interaction methods (Fig. S11F). It is important to note that it is easier to achieve larger size antigen-antibody complexes utilizing 20 nm AuNPs, therefore we were able observe bigger clusters at the same antigen concentration in the sample. Furthermore, antigen binding ability and Fc stability of the antibodies post immobilization on AuNPs were investigated via a sandwich ELISA assay (Fig. S12). The results show similar trends for antibodies immobilized on 5 nm AuNPs. The UV-NBS method provides the best antigen binding ability and Fc stability of the antibodies on AuNP's surface. Since EDC-NHS method rely on conjugation to carboxylated AuNP surface through reactive amine chemistry at arbitrary lysine residues, highly disordered immobilization of antibodies will occur, leading non-active antibodies on the AuNP unable to bind the antigen and recognized by a Fc specific secondary antibody. For ionic interactions method, antibodies fail to remain on AuNPs' surface during washing steps of ELISA. For thiol reduction method, unsurprisingly, Fc specific secondary antibody fails to recognize the Fc part of the heavy chain of the reduced antibodies.

CONCLUSION

In this study, we demonstrate that UV-NBS method can be utilized to generate antibody functionalized AuNPs yielding significantly enhanced antigen detection efficiency and improved antigen binding sensitivity with high specificity when compared to three other commonly used antibody functionalization methods: EDC-NHS, thiol reduction and ionic interaction. Both the EDC-NHS and ionic interactions methods yield randomly oriented immobilization of antibodies and obstructing antigen binding site. Even though thiol reduction method uses specific thiol sites for oriented immobilization, high levels of antigen binding activity is typically not observed post immobilization possibly due to the harsh chemical conditions required for disulfide bond reduction causing damage to the antibody tertiary structure. The results presented in this study establish the UV-NBS method as a universal, gentle, practical and reproducible method for functionalization of antibodies with TA moieties in order to conjugate them with AuNPs in a site-specific manner for enhanced detection purposes.

This study also demonstrates a one-step PSA detection method that yields highly sensitive, specific and rapid results. Even though other methods, such as well-established Raman scattering or ELISA, can also sensitively detect PSA levels with even lower values of LOD[37,54], many of these methods require expertise in hi-tech equipment that are not possible to use in many third world countries. Furthermore, according to the National Cancer Institute (NCI), PSA levels of 5.0 ng/mL (~ 125 pM) or lower in the blood of healthy subjects are considered normal, which is well within the accurate detection range of this method. Additionally, the measurement of cluster formation of antibody functionalized AuNPs via DLS to target PSA in the sample does not require any washing or blocking steps; thus, can generate results within 10 min providing an easy detection method without any requirement of expertise in sophisticated experimental techniques or instrumentation. Long-term storage of the antibody functionalized AuNPs, however, still requires optimization for different conditions and temperatures, which is currently being investigated in our labs. This study provides the proof of concept for the utilization of antibody functionalized AuNPs via the UV-NBS method in a one-step diagnostic application, and that can be implemented to many other detection systems. Since NBS is a universal site conserved on all antibody Fab, we anticipate that other antibody fragments such as Fab, Fab_2, Fab´, and ScFv that contain an NBS site can also be functionalized utilizing the UV-NBS method. The UV-NBS method can also be utilized for site-specific functionalization of antibodies with a variety of molecules carrying an IBA-moiety; hence, oriented immobilization of antibodies can be applied to other nanoparticle platforms such as iron oxide nanoparticles, quantum dots and up-converting nanoparticles, which are currently being evaluated in our laboratories, to be used in enhanced biosensing applications. Taken together, antibody functionalized AuNPs via the UV-NBS method has exceptional potential to be used in numerous diagnostic and therapeutic applications with numerous advantages especially in the design of small-scale sensor diagnostics, microfluidic devices and living cell systems.

Supplementary Material

Refer to Web version on PubMed Central for supplementary material.

Acknowledgments

This work was supported by the National Science Foundation (NSF) (grant award number CBET – 1263713) and the National Institutes of Health (NIH) (grant award number R01AI108884). NM is supported by a Berry Family Foundation Fellowship from the Advanced Diagnostics and Therapeutics Initiative at the University of Notre Dame.

The authors thank the Center for Environmental Science and Technology for usage of the DLS, as well as the University of Notre Dame Mass Spectrometry and Proteomics Facility for the usage of mass analysis instrumentation.

References

1. Lisa M, Chouhan R, Vinayaka A, Manonmani H, Thakur M. Biosensors and Bioelectronics. 2009; 25:224–227. [PubMed: 19576759]
2. Sokolov K, Follen M, Aaron J, Pavlova I, Malpica A, Lotan R, Richards-Kortum R. Cancer Res. 2003; 63:1999–2004. [PubMed: 12727808]
3. Wilson R. Chem Soc Rev. 2008; 37:2028–2045. [PubMed: 18762845]

4. Marega R, Karmani L, Flamant L, Nageswaran PG, Valembois V, Masereel B, Feron O, Vander Borght T, Lucas S, Michiels C. Journal of Materials Chemistry. 2012; 22:21305–21312.
5. Gao J, Huang X, Liu H, Zan F, Ren J. Langmuir. 2012; 28:4464–4471. [PubMed: 22276658]
6. Kogan MJ, Bastus NG, Amigo R, Grillo-Bosch D, Araya E, Turiel A, Labarta A, Giralt E, Puntes VF. Nano Letters. 2006; 6:110–115. [PubMed: 16402797]
7. El-Sayed IH, Huang X, El-Sayed MA. Cancer Lett. 2006; 239:129–135. [PubMed: 16198049]
8. Dreifuss T, Betzer O, Shilo M, Popovtzer A, Motiei M, Popovtzer R. Nanoscale. 2015; 7:15175–15184. [PubMed: 26313344]
9. Muthu MS, Agrawal P, Singh S. Nanomedicine. 2016; 11:327–330. [PubMed: 26784106]
10. Giljohann DA, Seferos DS, Daniel WL, Massich MD, Patel PC, Mirkin CA. Angewandte Chemie International Edition. 2010; 49:3280–3294. [PubMed: 20401880]
11. Chen W, Luo G, Xu X, Jia H, Lei Q, Han K, Zhang X. Nanoscale. 2014; 6:9531–9535. [PubMed: 24989070]
12. Treguer-Delapierre M, Majimel J, Mornet S, Duguet E, Ravaine S. Gold Bulletin. 2008; 41:195–207.
13. Gagner JE, Qian X, Lopez MM, Dordick JS, Siegel RW. Biomaterials. 2012; 33:8503–8516. [PubMed: 22906603]
14. Perassi EM, Hrelescu C, Wisnet A, Döblinger M, Scheu C, Jäckel F, Coronado EA, Feldmann J. ACS nano. 2014; 8:4395–4402. [PubMed: 24787120]
15. Su S, Zou M, Zhao H, Yuan C, Xu Y, Zhang C, Wang L, Fan C, Wang L. Nanoscale. 2015; 7:19129–19135. [PubMed: 26524543]
16. Saha K, Agasti SS, Kim C, Li X, Rotello VM. Chem Rev. 2012; 112:2739–2779. [PubMed: 22295941]
17. Zheng T, Bott S, Huo Q. ACS Applied Materials & Interfaces. 2016; 8:21585–21594. [PubMed: 27472008]
18. Omidfar K, Khorsand F, Azizi MD. Biosensors and Bioelectronics. 2013; 43:336–347. [PubMed: 23356999]
19. van der Heide S, Russell DA. J Colloid Interface Sci. 2016; 471:127–135. [PubMed: 26994353]
20. Ackerson CJ, Jadzinsky PD, Jensen GJ, Kornberg RD. J Am Chem Soc. 2006; 128:2635–2640. [PubMed: 16492049]
21. Busseron E, Ruff Y, Moulin E, Giuseppone N. Nanoscale. 2013; 5:7098–7140. [PubMed: 23832165]
22. Sperling RA, Gil PR, Zhang F, Zanella M, Parak WJ. Chem Soc Rev. 2008; 37:1896–1908. [PubMed: 18762838]
23. Li Z, Jin R, Mirkin CA, Letsinger RL. Nucleic Acids Res. 2002; 30:1558–1562. [PubMed: 11917016]
24. Oh E, Susumu K, Blanco-Canosa J, Medintz I, Dawson P, Mattoussi H. Small. 2010; 6:1273–1278. [PubMed: 20486227]
25. Day ES, Bickford LR, Slater JH, Riggall NS, Drezek RA, West JL. Int J Nanomedicine. 2010; 5:445–454. [PubMed: 20957166]
26. Thobhani S, Attree S, Boyd R, Kumarswami N, Noble J, Szymanski M, Porter RA. J Immunol Methods. 2010; 356:60–69. [PubMed: 20188107]
27. Gray JJ. Curr Opin Struct Biol. 2004; 14:110–115. [PubMed: 15102457]
28. Yoshimoto K, Nishio M, Sugasawa H, Nagasaki Y. J Am Chem Soc. 2010; 132:7982–7989. [PubMed: 20491483]
29. Tiwari PM, Vig K, Dennis VA, Singh SR. Nanomaterials. 2011; 1:31–63. [PubMed: 28348279]
30. Baniukevic J, Kirlyte J, Ramanavicius A, Ramanaviciene A. Sensors Actuators B: Chem. 2013; 189:217–223.
31. Kausaite-Minkstimiene A, Ramanaviciene A, Kirlyte J, Ramanavicius A. Anal Chem. 2010; 82:6401–6408. [PubMed: 20669994]
32. Lee JM, Park HK, Jung Y, Kim JK, Jung SO, Chung BH. Anal Chem. 2007; 79:2680–2687. [PubMed: 17341056]

33. Alves NJ, Mustafaoglu N, Bilgicer B. Bioconjug Chem. 2014; 25:6534–6541.
34. Alves NJ, Champion MM, Stefanick JF, Handlogten MW, Moustakas DT, Shi Y, Shaw BF, Navari RM, Kiziltepe T, Bilgicer B. Biomaterials. 2013; 34:5700–5710. [PubMed: 23601661]
35. Alves NJ, Mustafaoglu N, Bilgicer B. Biosens Bioelectron. 2013; 49:387–393. [PubMed: 23800610]
36. Alves NJ, Kiziltepe T, Bilgicer B. Langmuir. 2012; 28:9640–9648. [PubMed: 22612330]
37. Mustafaoglu N, Alves NJ, Bilgicer B. Langmuir. 2015; 31:9728–9736. [PubMed: 26273992]
38. Mustafaoglu N, Alves NJ, Bilgicer B. Biotechnol Bioeng. 2015; 112:1327–1334. [PubMed: 25678249]
39. Handlogten MW, Kiziltepe T, Moustakas DT, Bilgicer B. Chem Biol. 2011; 18:1179–1188. [PubMed: 21944756]
40. Handlogten MW, Serezani AP, Sinn AL, Pollok KE, Kaplan MH, Bilgicer B. J Immunol. 2014; 192:2035–2041. [PubMed: 24489096]
41. Handlogten MW, Kiziltepe T, Serezani AP, Kaplan MH, Bilgicer B. Nat Chem Biol. 2013; 9:789–795. [PubMed: 24096304]
42. Sutcliffe S, Pakpahan R, Sokoll LJ, Elliott DJ, Nevin RL, Cersovsky SB, Walsh PC, Platz EA. BJU Int. 2012; 110:1627–1635. [PubMed: 22502603]
43. Moyer VA, US Preventive Serv Task Force. Ann Intern Med. 2012; 157:120–134. [PubMed: 22801674]
44. Parolo C, de la Escosura-Muñiz A, Polo E, Grazú V, de la Fuente, Jesús M, Merkoçi A. ACS applied materials & interfaces. 2013; 5:10753–10759. [PubMed: 24095174]
45. Guirgis BS, Cunha CSe, Gomes I, Cavadas M, Silva I, Doria G, Blatch GL, Baptista PV, Pereira E, Azzazy HM. Analytical and bioanalytical chemistry. 2012; 402:1019–1027. [PubMed: 22089818]
46. Sharma H, Mutharasan R. Anal Chem. 2013; 85:2472–2477. [PubMed: 23356211]
47. Alves NJ, Cusick W, Stefanick JF, Ashley JD, Handlogten MW, Bilgicer B. Analyst. 2013; 138:4746–4751. [PubMed: 23841107]
48. Palik, ED. Handbook of optical constants of solids. Academic press; 1998.
49. Pattison DI, Rahmanto AS, Davies MJ. Photochemical & Photobiological Sciences. 2012; 11:38–53. [PubMed: 21858349]
50. Han HJ, Kannan RM, Wang S, Mao G, Kusanovic JP, Romero R. Adv Funct Mater. 2010; 20:409–421. [PubMed: 26290658]
51. Phillips A, Shaper AG, Whincup P. The Lancet. 1989; 334:1434–1436.
52. Stites SW, Nelson ME, Wesselius LJ. CHEST Journal. 1995; 107:1681–1685.
53. McPherson, RA., Pincus, MR. Henry's clinical diagnosis and management by laboratory methods. Elsevier Health Sciences; 2011.
54. Grubisha DS, Lipert RJ, Park H, Driskell J, Porter MD. Anal Chem. 2003; 75:5936–5943. [PubMed: 14588035]

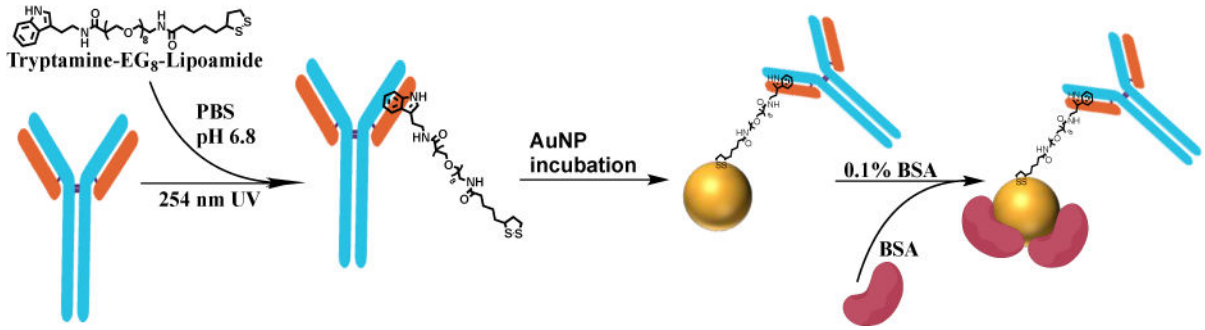

Fig. 1.

Schematic representation of antibody functionalization with tryptamine-EG_8-TA ligand utilizing the UV-NBS method, followed by conjugation of TA-functionalized antibody on 5 nm AuNPs surface.

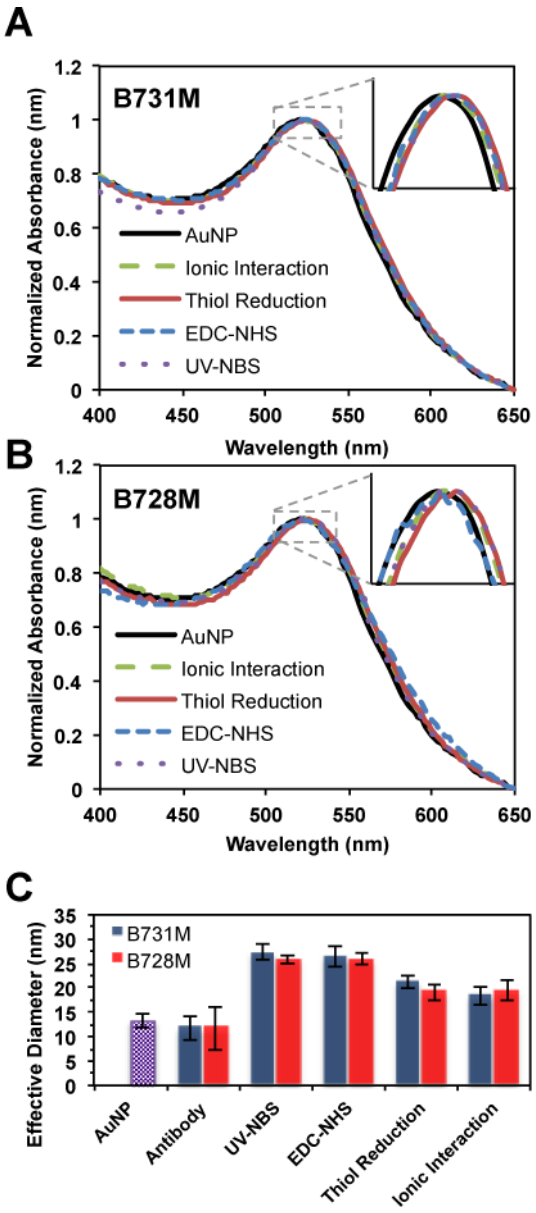

Fig. 2.

Absorbance spectra of AuNPs before (black line) and after functionalization with two different PSA specific antibodies: **A)** B731M and **B)** B728M via the ionic interaction, thiol reduction, EDC-NHS and UV-NBS methods, indicating successful functionalization of AuNPs with antibodies for all four methods without causing any aggregation. **C)** DLS measurements of AuNPs (purple bar), non-functionalized antibodies, and PSA specific antibody functionalized AuNPs via the UV-NBS, EDC-NHS, thiol reduction and ionic interaction methods.

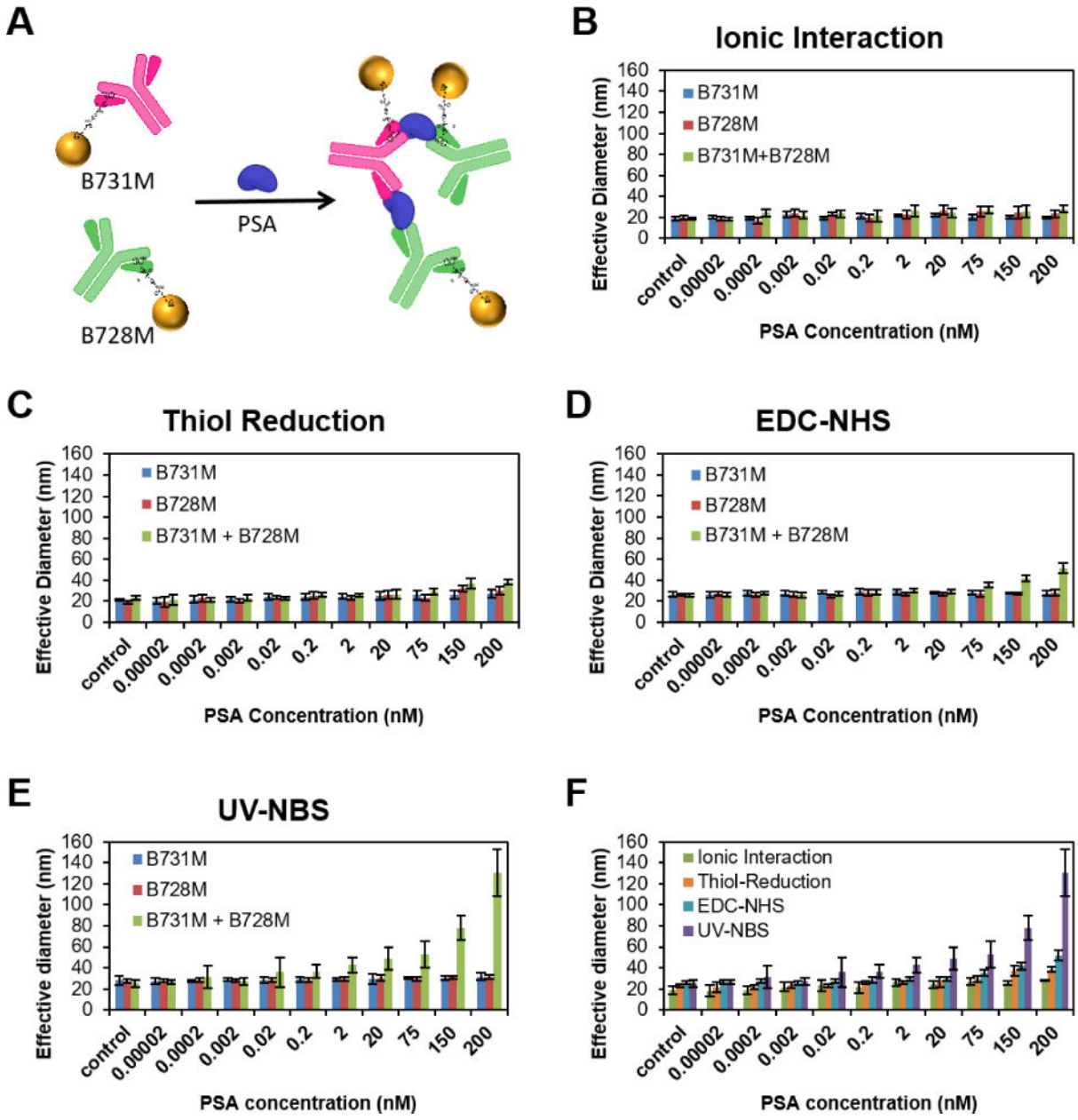

Fig. 3.

A) Schematic representation of antibody functionalized AuNPs' cluster formation upon binding of antigen. Antigen detection sensitivity of the antibody functionalized AuNPs prepared utilizing the **B)** ionic interaction, **C)** thiol reduction, **D)** EDC-NHS, and **E)** UV-NBS methods, was determined with DLS measurements. Size of the antibody functionalized AuNPs was measured with DLS upon addition of increasing concentrations of PSA. As expected, the size of AuNPs functionalized with only one antibody, either B731M (blue bar) or B728M (red bar), did not change whereas mixture of B731M and B728M functionalized AuNPs (green bar) formed clusters upon addition of increasing concentration of PSA (**F)** Comparison of cluster formations (green bars from B, C, D and E) utilized with all methods:

UV-NBS (purple), EDC-NHS (blue), Thiol Reduction (orange), and Ionic Interaction (green). All data represent means (±SD) of triplicate experiments.

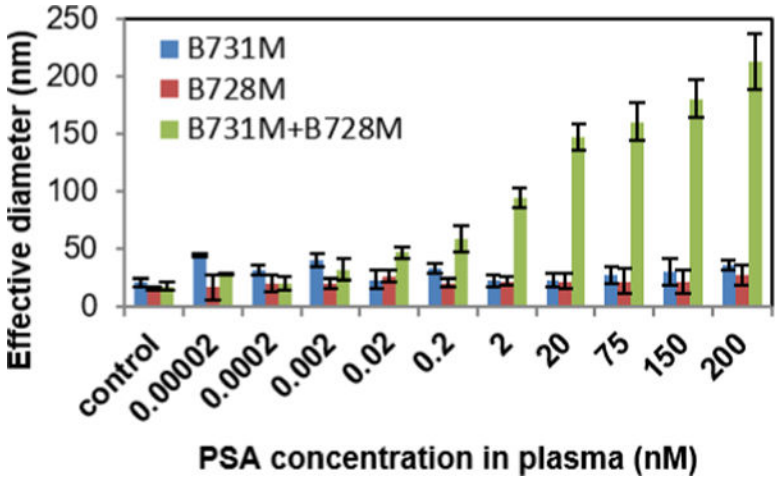

Fig. 4.

PSA detection in human serum utilizing antibody functionalized AuNPs prepared via the UV-NBS method. The results indicate a high sensitivity in detection of PSA in biological samples.

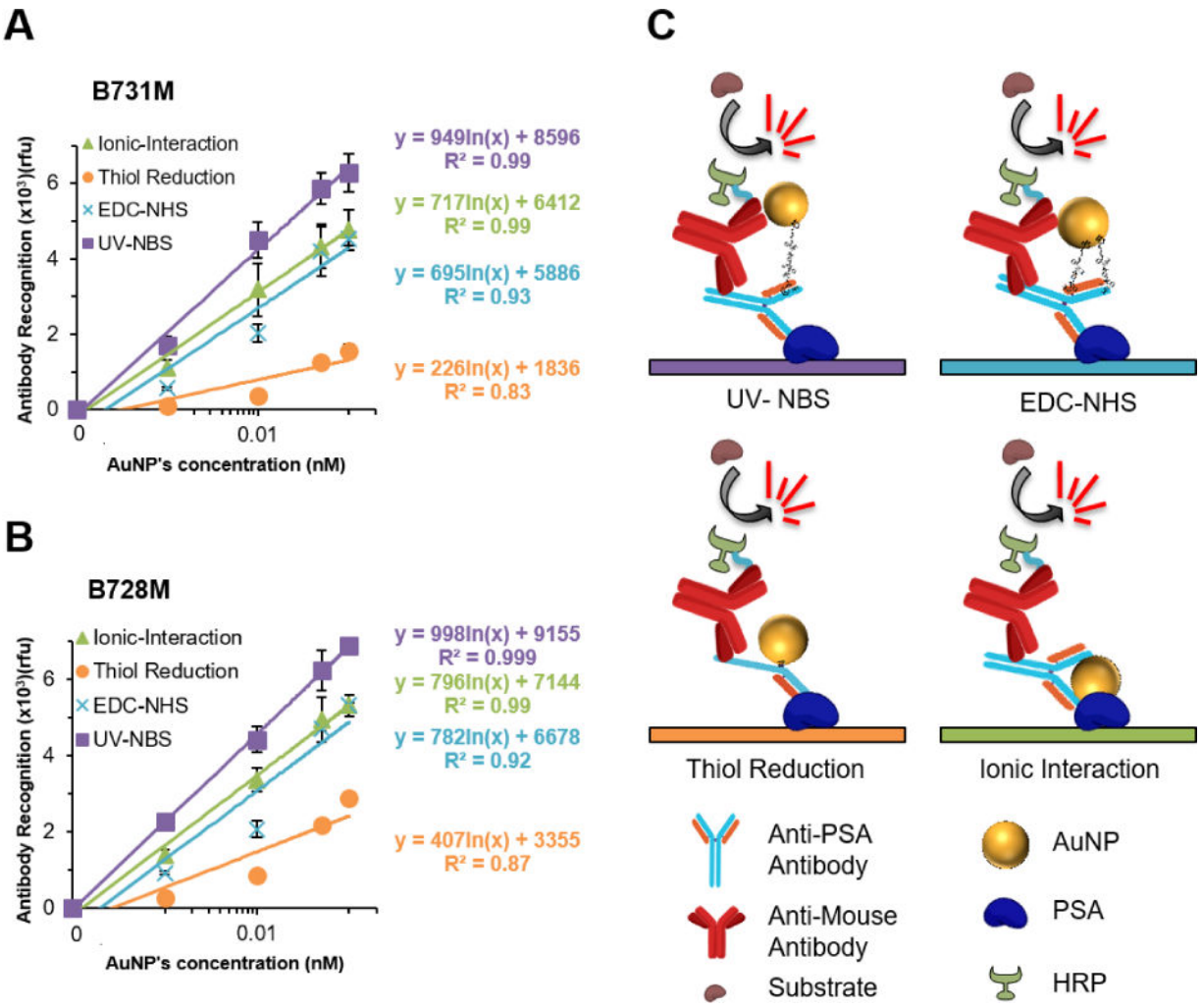

Fig. 5.

Comparison of the efficiencies for UV-NBS, EDC-NHS, thiol reduction and ionic interaction immobilization methods on AuNPs via ELISA assays for **A)** B731M and **B)** B728M antibody. **C)** Schematic representation of the ELISA used for each method determining antigen binding sensitivity and Fc stability of immobilized antibodies on AuNP surface. All data represent means (±SD) of triplicate experiments.

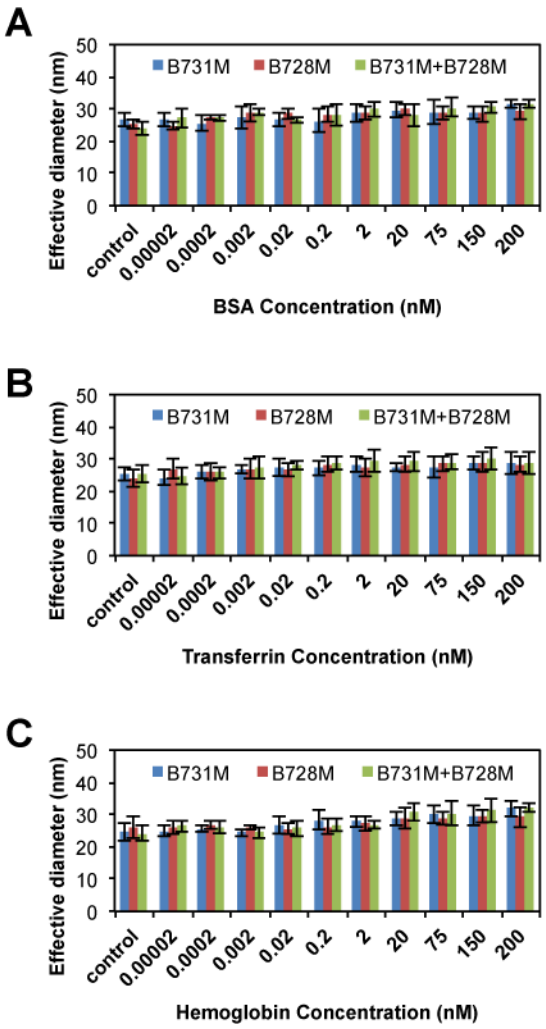

Fig. 6.

The specificity of the AuNP detection system prepared via the UV-NBS method was tested by measuring the cluster formation of AuNPs that are functionalized with PSA specific antibodies; B731M and B728M in the presence of non-specific targets such as **A)** BSA, **B)** transferrin, and **C)** hemoglobin instead of PSA. As expected, cluster formation was not observed, with non-specific protein targets utilizing anti-PSA immobilized AuNPs.

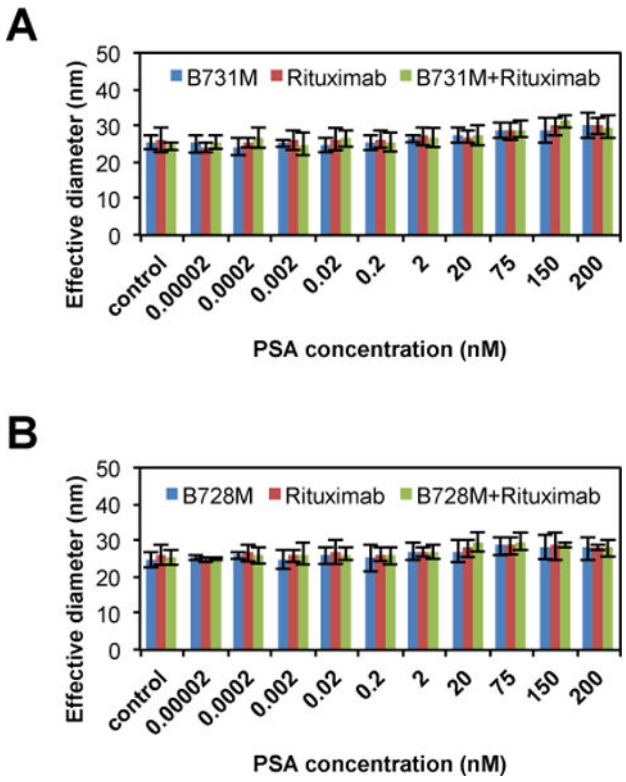

Fig. 7.

AuNPs were conjugated with Rituximab, anti-CD20 antibody, to validate the selectivity of the antibody functionalized AuNP detection system against to PSA target. Sandwich assays were carried out utilizing one of anti-PSA antibody functionalized AuNPs, either **A)** B731M or **B)** B728M, and Rituximab functionalized AuNP to target PSA. Results show that there are no non-specific interactions.

Table 1

The limit of detection (LOD) values for PSA utilizing antibody functionalized AuNPs generated with various methods: UV-NBS, EDC-NHS, thiol reduction and ionic interaction.

	LOD (nM)
UV-NBS	0.055
EDC-NHS	2.2
Thiol Reduction	46.8
Ionic Interaction	323.0